

## Nanostructured Screen-Printed Electrodes Modified with Self-Assembled Monolayers for Determination of Metronidazole in Different Matrices

Bryan C. Huayhuas-Chipana,<sup>a,c</sup> Juan C. M. Gomero<sup>a,b</sup> and Maria D. P. T. Sotomayor<sup>\*,c</sup>

<sup>a</sup>Facultad de Ciencias, Universidad Nacional de Ingeniería, Av. Túpac Amaru 210, Lima, Peru

<sup>b</sup>Facultad de Ingeniería Industrial, Universidad de Lima, Santiago de Surco, Lima, Peru

<sup>c</sup>Departamento de Química Analítica, Instituto de Química,  
Universidade Estadual Paulista (UNESP), 14800-110 Araraquara-SP, Brazil

Neste trabalho é descrito o desenvolvimento de um sensor para detecção de metronidazol, usando um método simples para preparar estruturas nanoporosas de ouro em eletrodos impressos comerciais modificados com monocamadas autoarranjadas de tiol (SAMs). O processo envolve a formação inicial de espécies de ouro oxidadas a pH 7,0, e posteriormente a redução potenciodinâmica para a formação da superfície nanoestruturada, que a seguir foi modificada com cisteína para obtenção do sensor, o qual foi posteriormente caracterizado utilizando microscópio eletrônico de varredura (SEM), microscópio de força atômica (AFM) e técnicas eletroquímicas. Para a quantificação de metronidazol foi otimizada a voltametria de onda quadrada (SWV). Nas melhores condições de análise o sensor mostrou em  $-0,36$  V uma faixa linear entre 50 e 300  $\mu\text{mol L}^{-1}$  e limite de detecção (LOD) = 2,6  $\mu\text{mol L}^{-1}$ . No estudo de seletividade, o eletrodo mostrou mais alta sensibilidade para os nitroimidazóis. A resposta do sensor indica ser viável para a detecção deste fármaco em diferentes tipos de matrizes.

This paper describes the development of a sensor for the determination of metronidazole using a simple method involving the creation of nanoporous structures on gold electrodes followed by modification with self-assembled monolayers (SAMs) of thiols. The initial formation of oxidized gold species at pH 7.0 was followed by potentiodynamic reduction in order to obtain a nanostructured surface that was then modified with a SAM of cysteine. The sensor was characterized by scanning electron microscopy (SEM), atomic force microscopy (AFM), and electrochemical techniques. Quantification of metronidazole was performed using optimized square wave voltammetry. Under the best analytical conditions, the sensor operated at  $-0.36$  V showed a linear range of 50-300  $\mu\text{mol L}^{-1}$  and a limit of detection (LOD) of 2.6  $\mu\text{mol L}^{-1}$ . Evaluation of selectivity demonstrated that the electrode provided higher sensitivity towards nitroimidazoles. The sensor responses showed that it could be used for detection of metronidazole in different types of matrix.

**Keywords:** self-assembled monolayers, cysteine, metronidazole, nanostructured gold electrode

### Introduction

It is well known that gold reacts with sulfur to form thermodynamically and kinetically stable self-assembled monolayers (SAM) that are widely used in the manufacture of sensors and biosensors, where they act as molecular electronic biointerfaces.<sup>1-16</sup> Thiols<sup>17,18</sup> are used to improve the stability of these devices and to transfer analyte redox information to the metal surface. Gold electrodes with greater porosity can be produced by electrochemical

deposition.<sup>19</sup> Au-Ag alloys have also been used as starting materials for the preparation of porous gold electrodes, where a relatively complex procedure is used to fuse gold with silver for subsequent separation.<sup>20-25</sup>

Nitro-containing compounds are widely found as byproducts in industrial processes such as those used to manufacture agrochemicals, dyes, and pharmaceuticals. Among the various nitro compounds, nitroimidazoles are some of the most common co-products. These compounds exhibit selective activity against anaerobic microorganisms, enabling them to be used in the treatment of infectious diseases in humans and animals.<sup>26</sup> However, the same

\*e-mail: mpilar@iq.unesp.br

compounds employed to combat microbial infections also show genotoxicity, which can cause adverse health effects including decreased fertility rates, mutagenesis, and carcinogenesis.<sup>27-30</sup>

The drug metronidazole is a nitro compound that is widely used due to its antiprotozoal properties and its activity against anaerobic gram-negative bacilli, gram-positive spore-forming bacilli, and all anaerobic cocci. The drug is widely indicated for the treatment of giardiasis, amoebiasis, *Trichomoniasis vaginitis*, *Gardnerella vaginalis*, and infections caused by anaerobic bacteria such as *Bacteroides fragilis* and other *Bacteroides* spp., *Fusobacterium* spp., *Clostridium* spp., *Eubacterium* spp., and anaerobic cocci. It is used to treat patients with refractory chronic periodontitis, a disease characterized by the presence of anaerobic bacteria in the oral cavity. It is possible for the drug to be excreted and released to the environment in domestic sewage, making it an emerging pollutant that deserves attention due to the known adverse health effects of nitro compounds.

Various sensors have been described for the determination of metronidazole (Table 1). However, sensor construction can be difficult<sup>34,35</sup> and response ranges are narrow.<sup>32-34,37</sup> It is therefore still necessary to develop reliable alternative analytical techniques for the determination of this and other nitro compounds present in biological and environmental samples.

The present work describes a new and simple procedure for producing a nanostructured gold electrode modified with a cysteine SAM for the determination of metronidazole in pharmaceutical formulations and biological samples.

**Table 1.** Different sensors reported for the detection of metronidazole

Composition of the sensing phase	Working electrode	Reference electrode	Linear range / (mol L <sup>-1</sup> )	LOD / (mol L <sup>-1</sup> )	Ref.
Thin film nanostructure of Mg/Fe - layered double hydroxides (Mg/Fe-LDH)	Glassy carbon electrode (GCE)	SCE	$3.0 \times 10^{-6}$ - $1.0 \times 10^{-3}$	–	31
Gold nanotubes (GNT)	Carbon paste electrode	Ag/AgCl	$0.2 \times 10^{-6}$ - $2.0 \times 10^{-6}$	$0.10 \times 10^{-9}$	32
Magnetic molecularly imprinted polymer (MMIP/MGCE)	Magnetic glassy carbon electrode (MGCE)	SCE	$0.05 \times 10^{-6}$ - $1.0 \times 10^{-6}$	$0.016 \times 10^{-6}$	33
Graphene and ionic liquid (IL) of 1-butyl-3-methylimidazolium hexafluorophosphate (BMIMPF <sub>6</sub> ) composite	Glassy carbon electrode	SCE	$0.1 \times 10^{-6}$ - $25.0 \times 10^{-6}$	$0.047 \times 10^{-6}$	34
Cysteic acid and graphene functionalized with poly(diallyldimethylammonium chloride)	Glassy carbon electrode	SCE	$0.01 \times 10^{-6}$ - $1.0 \times 10^{-6}$	$2.30 \times 10^{-9}$	35
Molecularly imprinted polymer (MIP)	Carbon paste electrode	Ag/AgCl	$0.32 \times 10^{-9}$ - $4.4 \times 10^{-6}$	$2.09 \times 10^{-10}$	36
Fiber microdisk electrode	Carbon microdisk	SCE	$5.0 \times 10^{-6}$ - $16 \times 10^{-6}$	$0.50 \times 10^{-6}$	37
Self-assembled monolayer cysteine SAM	Screen-printed nanostructured gold electrode	Silver	$50 \times 10^{-6}$ - $3.0 \times 10^{-4}$	$2.60 \times 10^{-6}$	This work

LOD: limit of detection

## Experimental

### Reagents

All the reagents and solvents used in this work were analytical or HPLC grade. A standard solution of metronidazole (MTZ) at a concentration of  $7.2 \times 10^{-3}$  mol L<sup>-1</sup> was prepared by dissolving a precisely weighed out quantity of the analyte in ethanol/water (1:4, v/v). Different concentrations were then prepared by diluting aliquots of the stock standard solution in Britton-Robinson (BR) buffer at pH 2.0 (used as the electrolyte). All aqueous solutions were prepared using deionized water (18.1 MΩ cm at 25 °C) obtained from a Milli-Q system (Millipore). The pH adjustment employed a pH meter (mPA 210, Tecnocon).

### Electrochemical measurements

The electrochemical measurements were performed using a potentiostat (PGSTAT 12, Autolab/Eco Chemie) coupled to a personal computer and controlled by GPES software (v. 4.9.006, Eco Chemie). A conventional electrochemical cell (15 mL volume) containing 3 electrodes was used. The reference electrode was a commercial Ag|AgCl electrode (Analion), a coil of platinum was used as the counter electrode, and a modified commercial gold SPE (DropSens 220BT, geometrical area of 0.126 cm<sup>2</sup>) was used as the working electrode.

All experiments were carried out at ambient temperature and anaerobic conditions were maintained by bubbling nitrogen through the solutions during the measurements.

## Preparation and modification of the nanostructured gold electrodes

The gold SPE was first treated in an aqueous solution of  $\text{H}_2\text{SO}_4$  ( $1.0 \times 10^{-4} \text{ mol L}^{-1}$ ) to clean the electrode surface, using a cyclic voltammetry potential between  $-0.6$  and  $0.8 \text{ V vs. Ag|AgCl}$  (3 cycles) and a scan rate of  $100 \text{ mV s}^{-1}$ . In the next step, the gold electrode was treated in a solution of  $\text{KOH}$  ( $0.5 \text{ mol L}^{-1}$ ), with application of a previously optimized potential of  $2.0 \text{ V}$  for  $180 \text{ s}$ . This was immediately followed by a linear cathodic sweep between  $2.0$  and  $-0.2 \text{ V}$ , at  $50 \text{ mV s}^{-1}$ , in phosphate buffer solution (pH 7.0) obtaining the nanostructured electrodes. All steps were carefully optimized to get oxidized gold surfaces without destroying the thin gold film covering the working electrode of the SPEs.

The nanostructured electrodes were characterized by scanning electron microscopy (SEM) and atomic force microscopy (AFM).

The sensors were obtained by immersing the nanostructured electrodes in  $0.1 \times 10^{-3} \text{ mol L}^{-1}$  cysteine solution for  $10 \text{ min}$ ,  $20 \text{ min}$ ,  $60 \text{ min}$ ,  $12 \text{ h}$ , and  $72 \text{ h}$ , in order to optimize formation of the SAM on the electrode surface. The best immersion time was found to be  $20 \text{ min}$ , which was then used in all subsequent preparation procedures.

## Application of the sensor using pharmaceutical formulations

Sample preparation was performed as described in the British Pharmacopoeia.<sup>38</sup> A lotion (containing a labeled amount of MTZ of  $100 \text{ mg g}^{-1}$ ) was prepared for analysis by weighing out  $61.1 \text{ mg}$  of the sample and adding  $2.5 \mu\text{L}$  of  $\text{H}_2\text{SO}_4$  ( $0.1 \text{ mmol L}^{-1}$ ) and  $3 \text{ mL}$  of methanol. The mixture was heated at  $40 \text{ }^\circ\text{C}$  until dissolution was complete, and then filtered. Finally, the volume was completed to  $50.0 \text{ mL}$  with a 1:4 (volume ratio) mixture of ethanol and aqueous BR buffer solution (pH 2.0).

A suspension of the drug (containing a labeled concentration of  $40 \text{ mg mL}^{-1}$  of benzoylmetronidazole) was prepared for analysis using  $2.2 \text{ mL}$  of sample, to which was added a solution of ethanol/water (1:4, v/v). The mixture was sonicated for several minutes, filtered, and the volume was completed to  $50.0 \text{ mL}$  using the ethanol/water solution (1:4, v/v).

For the analysis of tablets containing  $250 \text{ mg}$  of MTZ (labeled amount),  $10$  tablets were ground and homogenized. Approximately  $92.1 \text{ mg}$  of this solid mixture was weighed out and dissolved in the ethanol/water solution (1:4, v/v), after which the mixture was sonicated for several minutes and then filtered. The volume was completed to  $50.0 \text{ mL}$  using the ethanol/water solution (1:4, v/v).

In all cases, the concentrations of MTZ in the prepared samples were  $7.2 \times 10^{-3} \text{ mol L}^{-1}$  (based on the labeled MTZ values). In order to perform the measurements in the linear range of the sensor,  $100 \mu\text{L}$  aliquots of these samples were added to the measurement cell ( $10.0 \text{ mL}$ ) and quantified by the standard additions method. The concentrations of metronidazole expected in the measurement cell were therefore  $72 \mu\text{mol L}^{-1}$ .

## Application of the sensor using biological samples

Determination of MTZ in biological samples employed human serum and urine enriched with  $1.98 \times 10^{-3}$  and  $7.20 \times 10^{-3} \text{ mol L}^{-1}$  of analyte, and then diluted  $\times 10$  with deionized water, without any pretreatment. The samples were added to the measurement cell and quantified by the standard additions method.

## Results and Discussion

### Nanostructured electrode characterization

The formation of nanopores on the gold electrode surface can be explained in the following way. Firstly, when the gold electrode was treated by chronoamperometry ( $2.0 \text{ V}$  for  $180 \text{ s}$ ) in an alkaline medium ( $0.5 \text{ mol L}^{-1} \text{ KOH}$ ), there was the formation of  $\text{Au}(\text{OH})_3/\text{AuO}_2$  species in equilibrium on its surface, as indicated in the Pourbaix diagram (Figure 1).<sup>39</sup> A subsequent linear cathodic sweep (from  $2.0$  to  $-0.2 \text{ V}$ , at  $50 \text{ mV s}^{-1}$ ) in a neutral solution (phosphate buffer at pH 7.0) resulted in reduction of these oxidized species to form gold metal ( $\text{Au}^0$ ), as also indicated in the Pourbaix diagram (Figure 1). These redox processes on the gold surface caused a change in morphology and the formation of nanopores. There was, therefore, an increase

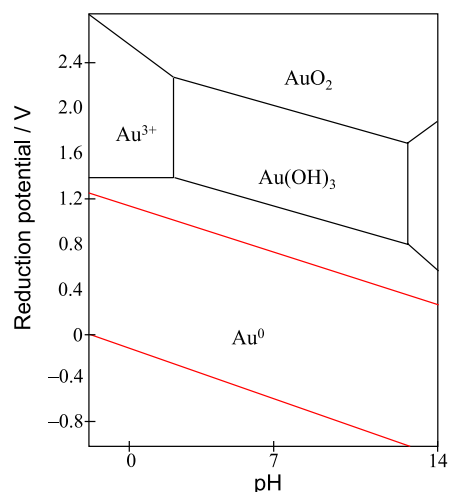


**Figure 1.** Pourbaix diagram for gold at  $25 \text{ }^\circ\text{C}$  (adapted from reference 39).

in the active area of the electrode surface, which enabled immobilization of greater amounts of catalytic species.

The increased surface areas of the gold electrodes after the treatment were evaluated using cyclic voltammetry (Figure 2). The active areas of untreated (bare) and nanostructured electrodes were estimated using the corresponding cathodic peak areas. These areas correspond to the removal of a monolayer of oxygen on the gold electrode surface, enabling the active area to be calculated using equation 1.<sup>40</sup>

$$Q = \frac{1}{\nu} \int_{T_i}^{T_f} IdE - Q_{dc} \quad (1)$$

where:  $Q$  is the total electrical charge;  $Q_{dc}$  is the electrical charge of the capacitive double layer;  $\nu$  is a constant specific to gold ( $400 \text{ mC cm}^{-2}$ ), and  $\int_{T_i}^{T_f} IdE$  corresponds to the active area of the electrode. The active areas of the two electrodes, calculated from the voltammograms shown in Figure 2, were  $0.138 \text{ cm}^2$  for the bare gold electrode (geometrical area  $0.126 \text{ cm}^2$ ) and  $3.205 \text{ cm}^2$  for the nanostructured electrode. The difference is evident in Figure 2, where the area of the cyclic voltammogram obtained for the nanostructured electrode is greater than for the untreated electrode. In addition, the nanostructured electrode showed an improvement in electronic transfer, since the difference between the anodic and cathodic peaks ( $138 \text{ mV vs. Ag|AgCl}$ ) was lower than for the untreated electrode ( $360 \text{ mV vs. Ag|AgCl}$ ).

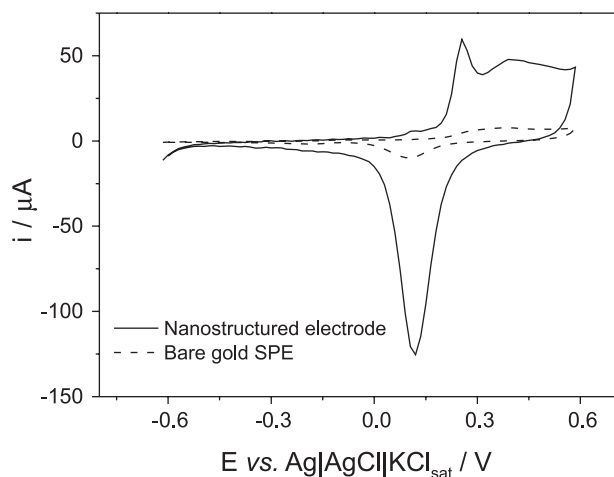


**Figure 2.** Cyclic voltammograms obtained for the untreated (dashed line) and nanostructured (solid line) screen-printed gold electrodes. Measurements carried out at  $50 \text{ mV s}^{-1}$  in  $1 \text{ mol L}^{-1} \text{ KOH}$ .

The morphology of the untreated (bare) and nanostructured electrodes was evaluated by SEM (Figure 3) and AFM (Figure 4). These analyzes clearly showed the formation of nanostructures on the electrode surface after treatment, in agreement with the cyclic voltammetry results. It is evident in Figure 3b that the nanoparticles

size is markedly different and can be explained due to the gold used in the SPE electrodes is polycrystalline. However, to obtain more homogeneous nanostructures, monocrystalline gold electrodes could be used (which can become expensive sensor) or using polycrystalline gold electrodes with preferential orientation in a single plane being this alternative economically more viable.

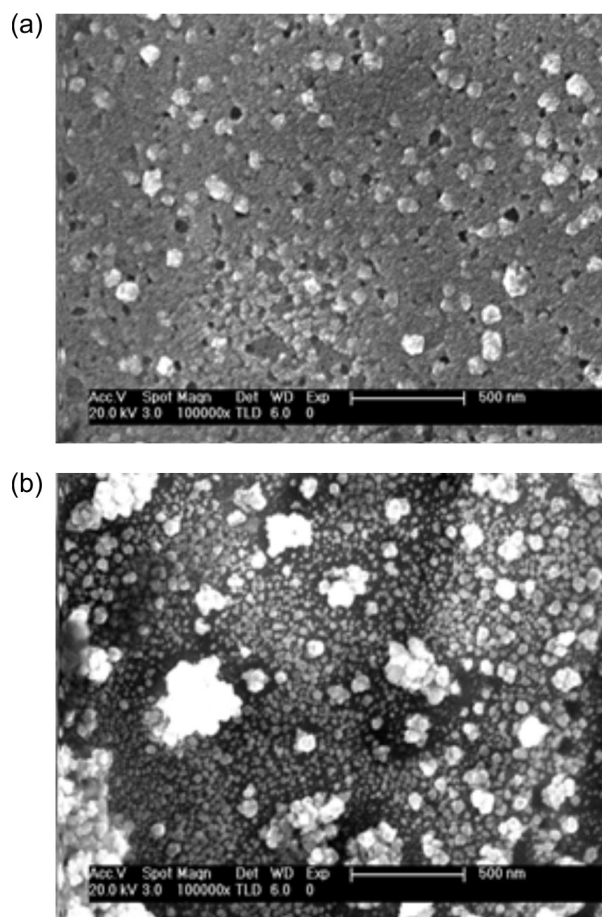


**Figure 3.** SEM images of the untreated (a) and nanostructured (b) screen-printed gold surfaces.

All these results indicated that the simple new gold treatment method was able to produce nanostructured electrodes that could be used to immobilize greater quantities of active molecules on their surfaces.

#### Modification of the nanostructured gold electrode with a cysteine SAM

Cyclic voltammetry experiments conducted from  $-1.2$  to  $0 \text{ V vs. Ag|AgCl}$ , in  $0.5 \text{ mol L}^{-1} \text{ KOH}$ , were used to confirm modification of the gold electrode nanostructure with the cysteine SAM. The results clearly revealed the presence of a cathodic peak at  $-0.7 \text{ V}$  (data not shown) that could be attributed to reductive desorption of the thiol on

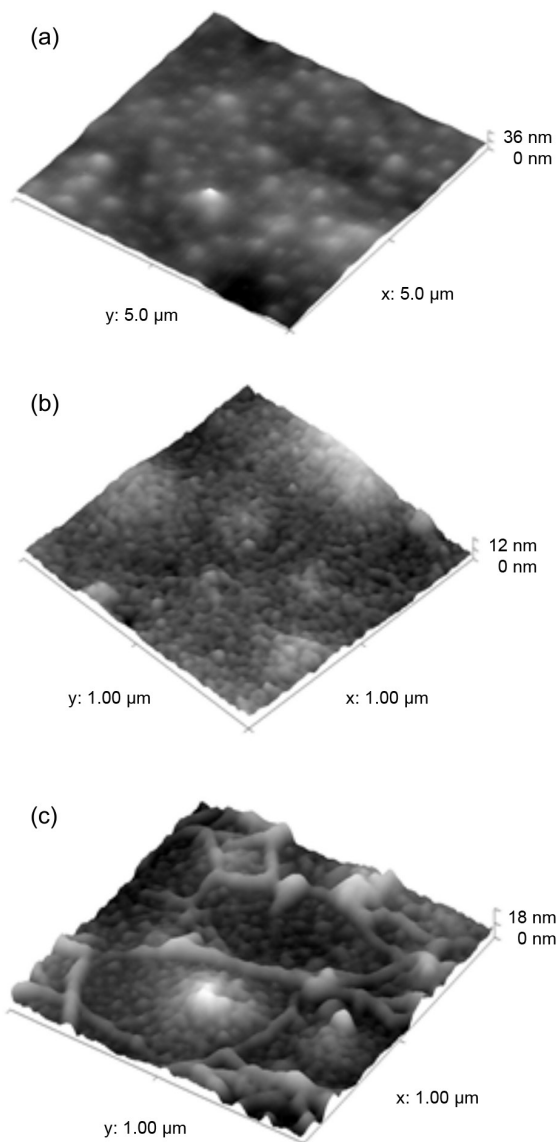


**Figure 4.** Atomic force microscopy images of untreated (a); nanostructured (b); and cysteine-modified nanostructured (c) screen-printed gold electrodes.

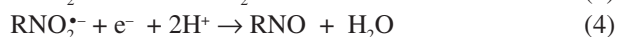
the gold surface, according to equation 2,<sup>41</sup> indicating the presence of cysteine on the electrode surface. This finding was supported by the AFM analysis (Figure 4c), which also demonstrated that the nanoporous electrode had been modified by the amino acid.



Based on the results obtained, Figure 5 shows a schematic representation of the formation of the SAM on the nanostructured gold electrode.

Characterization of the proposed sensor for nitro-containing compounds

After the construction of the sensor, the suitability of the sensor for use in pharmaceutical and/or environmental analyses was first evaluated by observing its response in the presence of different compounds containing the  $-\text{NO}_2$  group in their chemical structure. The study was based on the widely known reduction of  $-\text{NO}_2$  to  $-\text{NH}_2$ ,<sup>42-44</sup> according to the following reactions in an anaerobic medium:



The sensor response was tested using metronidazole and secnidazole, which belong to the nitroimidazole family of drugs, as well as *o*-nitrophenol, 1-chloro-2,4-dinitrobenzene, 4-nitro-*o*-phenylenediamine, and 2-nitro-*p*-phenylenediamine, which are potential environmental contaminants. All the cyclic voltammetry measurements were performed in anaerobic BR buffer solution (at pH 2.0) containing  $2.0 \times 10^{-4}$  mol L<sup>-1</sup> of each compound. The

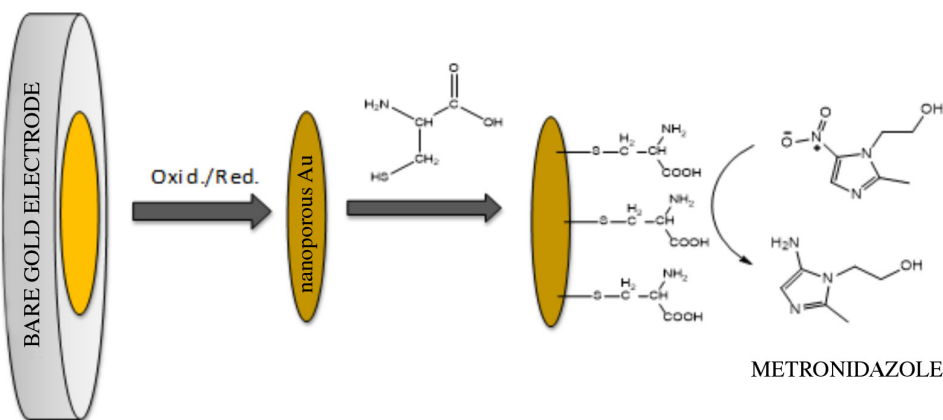


**Figure 5.** Schematic of the formation of a self-assembled monolayer of cysteine on the nanostructured screen-printed gold electrode.

voltammograms obtained for all the compounds (Figure 6) showed peaks corresponding to reduction of the nitro group,<sup>45</sup> although the peak profiles and values differed. For example, in the case of *o*-nitrophenol, a poorly-defined reduction peak only appeared at  $-350$  mV vs. Ag|AgCl, while for secnidazole and metronidazole, well-defined peaks appeared at  $-220$  mV vs. Ag|AgCl.

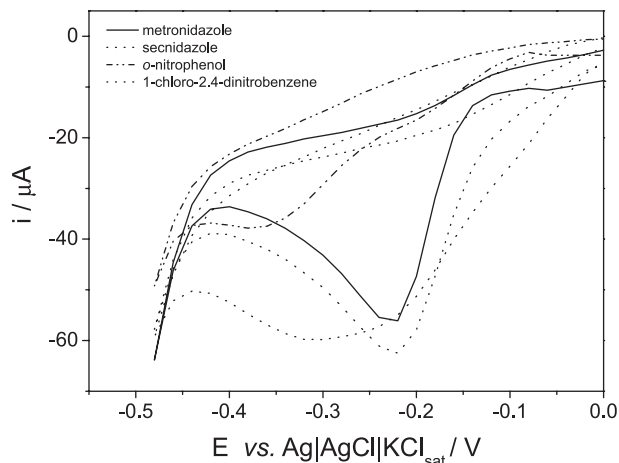
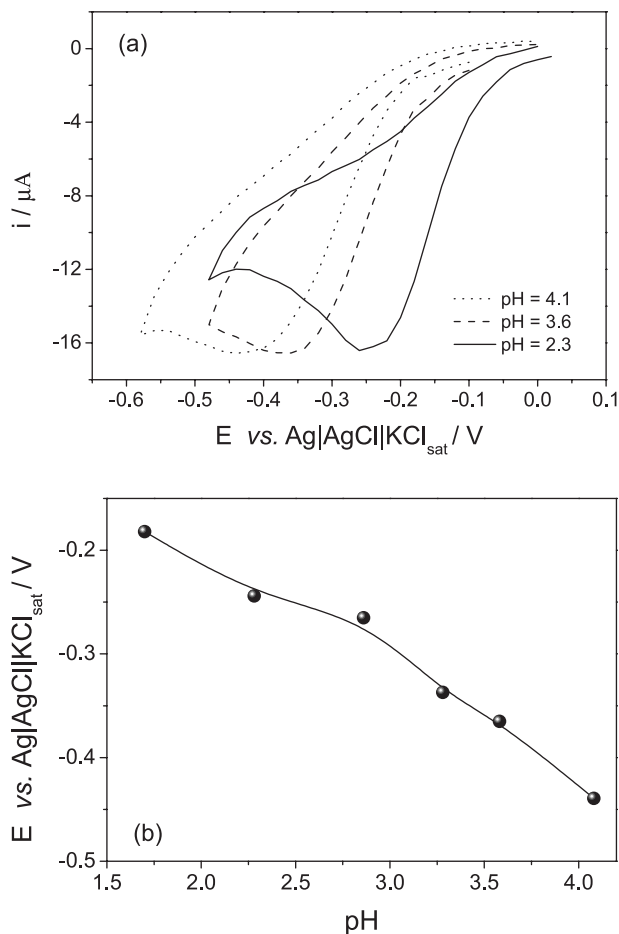


**Figure 6.** Cyclic voltammograms obtained using the proposed sensor in anaerobic BR buffer solution (pH 2.0) containing  $2.0 \times 10^{-4}$  mol L<sup>-1</sup> of different nitro-containing compounds. Scan rate: 100 mV s<sup>-1</sup>.

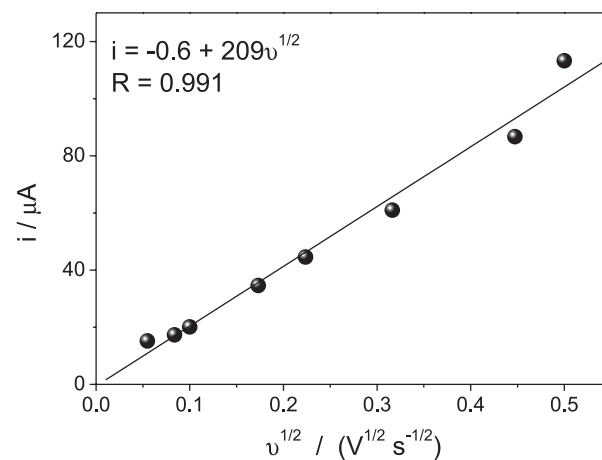
The potential application of the proposed sensor for the determination of metronidazole in pharmaceutical formulations was evaluated by considering its selectivity in the presence of other drugs. The compounds tested were lidocaine, diclofenac, and ranitidine, for which no responses were obtained in the same potential window, under the conditions selected for detection of MTZ. In the next step, it was therefore possible to optimize the analytical conditions in order to obtain the best response to MTZ. The reduction of MTZ is pH-dependent (reactions in equations 3-6), so pH was the first parameter considered in optimization of the sensor response.

Figure 7 shows the results obtained using 0.1 mol L<sup>-1</sup> BR buffer solution at different pH values between 1.6 and 4.0. It can be seen from Figure 7a that the pH did not influence the magnitude of the current obtained for the MTZ reduction. However, the peak potential shifted to less negative values as the pH decreased (Figure 7b). A pH of 2.0 was therefore selected for use in the subsequent experiments.

In the next step, evaluation was made of the influence of the scan rate ( $\nu$ ) on the cathodic potential peaks and the corresponding currents. The results of these experiments are shown in Figure 8, where the reduction current is plotted as a function of  $\nu^{1/2}$ . A linear fit was obtained, indicating that the reduction of MTZ was controlled by a mass transfer process.



**Figure 7.** Influence of pH on (a) current and (b) cathodic peak potential values. Measurements carried out at various pH values in 0.1 mol L<sup>-1</sup> BR buffer solutions containing  $2.0 \times 10^{-4}$  mol L<sup>-1</sup> MTZ.



**Figure 8.** Linear dependence of the cathodic peak current ( $i$ ) on the square root of the scan rate ( $\nu^{1/2}$ ), for cyclic voltammetry experiments carried out in anaerobic 0.1 mol L<sup>-1</sup> BR buffer solution (pH 2.0) containing  $2.0 \times 10^{-4}$  mol L<sup>-1</sup> of MTZ, using a potential window of 0 to  $-0.5$  V.

#### Characteristics of the proposed MTZ sensor

Application of the proposed sensor for the determination of MTZ in different samples was investigated using an

electroanalytical technique that was more sensitive than cyclic voltammetry. Among the techniques evaluated (amperometry, differential pulse voltammetry, and square wave voltammetry), square wave voltammetry (SWV) provided the best results. This technique was therefore optimized prior to its use to analyze the samples containing MTZ. The best SWV response was obtained at pulse amplitude of 100 mV, frequency of 60 Hz, and pulse increment of 10 mV. Typical voltammograms obtained under the optimized conditions are shown in Figure 9. The response to MTZ was linear in the range 50–300  $\mu\text{mol L}^{-1}$  ( $R = 0.9994$ ) and could be described by the equation:

$$\Delta i(\mu\text{A}) = 1.7 \times 10^{-6} (\pm 2.0 \times 10^{-7}) + 6.0 \times 10^{-2} (\pm 1.2 \times 10^{-3}) C_{\text{MTZ}} \quad (7)$$

The limits of detection (LOD) and quantification (LOQ) were 2.6 and 8.6  $\mu\text{mol L}^{-1}$ , respectively, calculated as recommended by the National Health Surveillance Agency (ANVISA).<sup>46</sup>

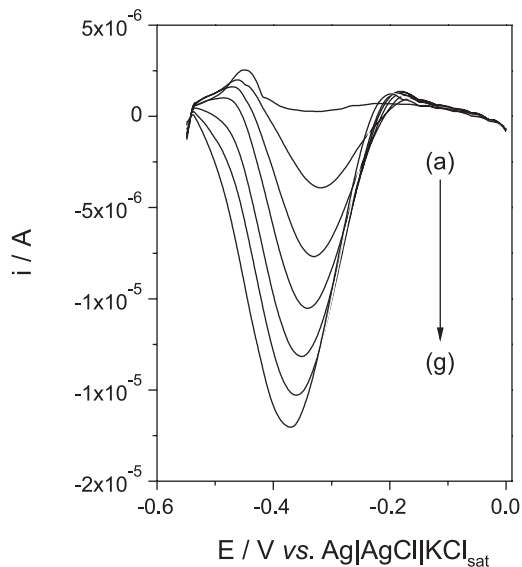


**Figure 9.** Response profile for MTZ obtained using SWV under optimized conditions. Measurements carried out in 0.1 mol L<sup>-1</sup> BR buffer (pH 2.0), with  $f = 60$  Hz,  $a = 100$  mV, and  $\Delta E = 10$  mV. (a) 0.1 mol L<sup>-1</sup> BR buffer alone; (b) 50  $\mu\text{mol L}^{-1}$  MTZ; (c) 101  $\mu\text{mol L}^{-1}$  MTZ; (d) 151  $\mu\text{mol L}^{-1}$  MTZ; (e) 199  $\mu\text{mol L}^{-1}$  MTZ; (f) 245  $\mu\text{mol L}^{-1}$  MTZ; (g) 295  $\mu\text{mol L}^{-1}$  MTZ.

The proposed sensor shows characteristics similar to other sensors described in literature, with the advantages of more simple preparation and possibility of miniaturization and mass construction.

#### Application of the proposed MTZ sensor

The results obtained for the application of the sensor in the analysis of different pharmaceutical formulations

are shown in Table 2. The response of the sensor in the presence of possible interferences was tested previously, and no effect on the MTZ signal was observed for substances including starch, mannitol, microcrystalline cellulose, povidone, magnesium stearate, cellulose acetate phthalate, talc, calcium carbonate, polyethylene glycol, and carbopol, which are used as excipients in commercial formulations.

**Table 2.** Results obtained using the proposed sensor for analysis of pharmaceutical formulations containing metronidazole

Formulation	Values obtained		
	Nominal	Found	Found/nominal / %
Tablet / (mg tablet <sup>-1</sup> )	250	245.3	98.1 ± 1.5
Drug suspension / (mg mL <sup>-1</sup> )	40 <sup>a</sup>	12.3	30.8 ± 0.1
Lotion / (mg g <sup>-1</sup> )	100	99.4	99.4 ± 2.3

<sup>a</sup>As benzoylmetronidazol.

Note that, in the case of suspension, the low recovery value is not due to the matrix effect, since the sample was pretreated as described in the experimental part, but due to the active ingredient of this drug is benzoylmetronidazole and not the analyte evaluated here (MTZ) for this proposed sensor.

The application of the sensor in the analysis of biological samples was tested by spiking urine and serum samples with MTZ. Excellent recovery values were achieved in both cases (Table 3). Possible interference from uric acid, urea, and ascorbic acid were evaluated, and no responses were observed for these compounds. However, in order to apply the sensor in the analysis of serum samples, and to avoid the effects of other potential interferences present in biological samples, the quantification of MTZ was carried out using the standard additions method. The results of these experiments confirmed the viability of the sensor for use with samples of clinical and pharmaceutical interest.

**Table 3.** Recovery values obtained using the proposed sensor in the analysis of biological samples

Sample	$C_{\text{Metronidazole}} / (\text{mol L}^{-1})$		Recovery / %
	Added	Found	
Urine	$7.20 \times 10^{-3}$	$6.72 \times 10^{-3}$	93.4 ± 0.8
Serum	$1.98 \times 10^{-3}$	$1.73 \times 10^{-3}$	89.3 ± 2.1

## Conclusions

This work presents a simple and novel method to obtain nanopores on the surface of gold electrodes. The presence

of the nanopores was confirmed using SEM, AFM, and cyclic voltammetry analyses. The procedure resulted in a higher surface area with a greater number of active sites available for immobilization of the amino acid cysteine, producing a sensor based on a self-assembled monolayer (SAM). This sensor is sensitive to molecules containing the nitro group in their structures. Metronidazole was chosen as a model drug, due to its clinical importance, and could be satisfactorily quantified in pharmaceutical formulations and biological samples.

## Acknowledgements

The authors gratefully acknowledge financial support from FAPESP (Proc. 2008/10449-7).

## References

- Saavedra, H. M.; Thompson, C. M.; Hohman, J. N.; Crespi, V. H.; Weiss, P.; *J. Am. Chem. Soc.* **2009**, *131*, 2252.
- Asadi, K.; Wu, Y.; Gholamrezaie, F.; Rudolf, P.; Bolm, P. W. M.; *Adv. Mater.* **2009**, *21*, 1.
- Chesneau, F.; Zhao, J.; Shen, C.; Buck, M.; Zharnikov, M.; *J. Phys. Chem. C* **2010**, *114*, 7112.
- Kang, H.; Lee, N. S.; Ito, E.; Hara, M.; Noh, J.; *Langmuir* **2010**, *114*, 2983.
- Kao, F.; Nepl, S.; Feulner, P.; Allara, D. L.; Zharnikov, M.; *J. Phys. Chem. C* **2010**, *114*, 13773.
- Seo, K.; Lee, Y.; *ACS Nano* **2009**, *3*, 2469.
- Alarcon, L. S.; Chen, L.; Esaulov, V. A.; Gayone, J. E.; Sanchez, E. A.; Grizzi, E. A.; *J. Phys. Chem. C* **2010**, *114*, 19993.
- Hamoudi, H.; Proto, M.; Dablemont, C.; Cavalleri, O.; Canepa, M.; Esaulov, V. A.; *Langmuir* **2010**, *26*, 7242.
- Azzam, W.; Bashir, A.; Terfort, A.; Strunskus, T.; Wöll, Ch.; *Langmuir* **2006**, *22*, 3647.
- Choi, Y.; Jeong, Y.; Chung, H.; Ito, E.; Hara, M.; Noh, J.; *Langmuir* **2008**, *24*, 91.
- Noh, J.; Jeong, Y.; Ito, E.; Hara, M.; *J. Phys. Chem. C* **2007**, *111*, 2691.
- Noh, J.; Kato, H. S.; Kawai, M.; Hara, M.; *J. Phys. Chem. B* **2002**, *106*, 13268.
- Choi, I.; Kang, H.; Lee, D.; Noh, J.; *Bull. Korean Chem. Soc.* **2012**, *33*, 381.
- Park, T.; Kang, H.; Kim, Y.; Lee, S.; Noh, J.; *Bull. Korean Chem. Soc.* **2011**, *32*, 39.
- McGuire, A.; Jewell, A. D.; Lawton, T. J.; Murphy, C. J.; Lewis, E. A.; Sykes, E. C. H.; *J. Phys. Chem. C* **2012**, *116*, 14992.
- Bellisario, D. O.; Jewell, A. D.; Tierney, H. L.; Baber, A. E.; Sykes, E. C. H.; *J. Phys. Chem. C* **2010**, *114*, 14583.
- Ruan, C.; Yang, F.; Lei, C.; Deng, D.; *Anal. Chem.* **1998**, *70*, 1721.
- Ganesh, V.; Pal, S. K.; Kumar, S.; Lakshminarayanan, V. J.; *Colloid Interface Sci.* **2006**, *296*, 195.
- Shin, H. C.; Dong, J.; Liu, M. L.; *Adv. Mater.* **2003**, *15*, 1610.
- Luo, H. M.; Sun, L.; Lu, Y. F.; Yan, Y. S.; *Langmuir* **2004**, *20*, 10218.
- Zhang, H.; Hussain, I.; Brust, M.; Cooper, A. I.; *AAAdv. Mater.* **2004**, *16*, 27.
- Walsh, D.; Arcelli, L.; Ikoma, T.; Mann, J. T.; *Nat. Mater.* **2003**, *2*, 386.
- Shchukin, D. G.; Caruso, R. A.; *Chem. Commun.* **2003**, 1478.
- Zhang, H.; Hussain, I.; Brust, M.; Butler, M. F.; Rannard, S. P.; Cooper, A. I.; *Nat. Mater.* **2005**, *4*, 787.
- Weissmuller, J.; Viswanath, R. N.; Kramer, D.; Zimmer, P.; Wurschum, R.; Gleiter, H.; *Science* **2003**, *300*, 312.
- Edwards, D. I.; *Prog. Med. Chem.* **1981**, *18*, 87.
- Bone, W.; Jones, N.; Kamp, G.; Yeung, C.; Cooper, T.; *J. Reprod. Fertil.* **2000**, *118*, 127.
- Menéndez, D.; Rojas, E.; Herrera, L.; Lopez, M.; Sordo, M.; Elizondo, G.; Ostrosky-Wegman, P.; *Mutat. Res.* **2001**, *478*, 153.
- Hrelia, P.; Fimognari, C.; Maffei, F.; Brighenti, B.; Garuti, L.; Burnelli, S.; Cantelli, G.; *Mutat. Res.* **1998**, *397*, 293.
- Trinh, S.; Reisset, G.; *Mutat. Res.* **1998**, *398*, 55.
- Nejati, K.; Asadpour-Zeynali, K.; *Mater. Sci. Eng., C* **2014**, *35*, 179.
- Mollamahale, Y. B.; Ghorbani, M.; Ghalkhani, M.; Vossoughi, M.; Dolati, A.; *Electrochim. Acta* **2013**, *106*, 288.
- Chen, D.; Deng, J.; Liang, J.; Xie, J.; Hu, C.; Huang, K.; *Sens. Actuators, B* **2013**, *183*, 594.
- Peng, J.; Hou, C.; Hu, X.; *Sens. Actuators, B* **2012**, *169*, 81.
- Liu, W.; Zhang, J.; Li, C.; Tang, L.; Zhang, Z.; Yang, M.; *Talanta* **2013**, *104*, 204.
- Gholivand, M. B.; Torkashvand, M.; *Talanta* **2011**, *84*, 905.
- Bartlett, P. N.; Ghoneim, E.; El-Hefnawy, G.; El-Hallag, I.; *Talanta* **2005**, *66*, 869.
- The British Pharmacopoeia*, 3<sup>rd</sup> ed.; London, UK, 2007.
- Van Muylder, J.; Pourbaix, M.; *Atlas of Electrochemical Equilibria in Aqueous Solutions*, 2<sup>nd</sup> English ed.; Marcel Pourbaix, National Association of Corrosion Engineers: New York, 1974.
- Bard, J. A.; Faulkner, L. R.; *Electrochemical Methods Fundamentals and Applications*, 2<sup>nd</sup> ed.; Dallas, 2001.
- Arihara, K.; Ariga, T.; Takashima, N.; Arihara, K.; Okajima, T.; Kitamura, F.; Tokuda, K.; Ohsaka, T.; *Phys. Chem. Chem. Phys.* **2003**, *5*, 3758.
- Bone, W.; Jones, N.; Kamp, G.; Yeung, C.; Cooper, T.; *J. Reprod. Fertil.* **2000**, *118*, 127.
- Viodé, C.; Battache, N.; Cenas, N.; Krauth-Siegel, L.; Chauviere, G.; Bakalara, N.; Perie, J.; *Biochem. Pharmacol.* **1999**, *57*, 549.

44. Mason, R. P.; Holtzman, J. L.; *Biochemistry* **1975**, *14*, 1626.
45. Shaofang, L.; Kangbing, W.; Xueping, D.; Shengshui, H.; *Talanta* **2004**, *63*, 653.
46. Agência Nacional de Vigilância Sanitária (ANVISA), Resolução 899 de 29 de maio de 2003, Guia para Validação de Métodos Analíticos e Bioanalíticos, Brasília, Brasil, 2003. [http://portal.anvisa.gov.br/wps/wcm/connect/4983b0004745975da005f43fbc4c6735/RE\\_899\\_2003\\_Determina+a+publica%C3%A7%C3%A3o+do+Guia+para+valida%C3%A7%C3%A3o+de+m%C3%A9todos+anal%C3%ADticos+e+bioanal%C3%ADticos.pdf?MOD=AJPERES](http://portal.anvisa.gov.br/wps/wcm/connect/4983b0004745975da005f43fbc4c6735/RE_899_2003_Determina+a+publica%C3%A7%C3%A3o+do+Guia+para+valida%C3%A7%C3%A3o+de+m%C3%A9todos+anal%C3%ADticos+e+bioanal%C3%ADticos.pdf?MOD=AJPERES). Accessed in July 2014.

*Submitted on: May 15, 2014*

*Published online: July 25, 2014*

**FAPESP has sponsored the publication of this article.**